

Path-independent integrals to identify localized plastic events in two dimensions

Mehdi Talamali,¹ Viljo Petäjä,¹ Damien Vandembroucq,^{1,2} and Stéphane Roux³

¹Unité Mixte CNRS–Saint-Gobain “Surface du Verre et Interfaces”, 39 Quai Lucien Lefranc, 93303 Aubervilliers cedex, France

²Laboratoire PMMH, ESPC, CNRS, Paris 6, Paris 7, 10 rue Vauquelin, 75231 Paris cedex 05, France

³LMT-Cachan, ENS de Cachan, CNRS-UMR 8535, Université Paris 6, PRES UniverSud, 61 avenue du Président Wilson, F-94235 Cachan cedex, France

(Received 28 January 2008; revised manuscript received 2 June 2008; published 22 July 2008)

We use a power expansion representation of plane-elasticity complex potentials due to Kolossov and Muskhelishvili to compute the elastic fields induced by a localized plastic deformation event. Far from its center, the dominant contributions correspond to first-order singularities of quadrupolar and dipolar symmetry which can be associated, respectively, with pure deviatoric and pure volumetric plastic strain of an equivalent circular inclusion. By construction of holomorphic functions from the displacement field and its derivatives, it is possible to define path-independent Cauchy integrals which capture the amplitudes of these singularities. Analytical expressions and numerical tests on simple finite-element data are presented. The development of such numerical tools is of direct interest for the identification of local structural reorganizations, which are believed to be the key mechanisms for plasticity of amorphous materials.

DOI: [10.1103/PhysRevE.78.016109](https://doi.org/10.1103/PhysRevE.78.016109)

PACS number(s): 62.20.F-, 46.15.-x, 02.30.Fn, 81.05.Kf

I. INTRODUCTION

The plasticity of amorphous materials has motivated an increasing amount of study in recent years. In the absence of an underlying crystalline lattice in materials such as foams, suspensions, or structural glasses, it is generally accepted that plastic deformation results from a succession of localized structural reorganizations [1–4]. Such changes of local structure release part of the elastic strain to reach a more favorable conformation and induce long-range elastic fields. The details of such local rearrangements and of the internal stress they induce obviously depend on the precise structure of the material under study, and its local configuration. However, the important observation is that outside the zone of reorganization *a linear elastic behavior prevails*. Therefore, elastic stresses can be decomposed onto a multipolar basis and, independently of the material details, it is possible to extract singular, scale-free, dominant terms which can be associated with a global pure deviatoric or pure volumetric local transformation of an equivalent circular inclusion. In particular, the elastic shear stress induced by a localized plastic shear exhibits a quadrupolar symmetry. This observation has motivated the development of statistical models of amorphous plasticity at the mesoscopic scale based upon the interaction of disorder and long-range elastic interactions [5–8]. In the same spirit, statistical models were also recently developed to describe the plasticity of polycrystalline materials [9]. Several numerical studies have been performed recently to identify these elementary localized plastic events in athermal or molecular dynamics simulations of model amorphous materials under shear [10,11].

The question remains of how to identify and analyze these transformation zones. In analogy with the path-independent Rice J integral [12] developed to estimate the stress intensity factor associated with a crack tip stress singularity, we aim here at capturing the stress singularity induced by the local plastic transformation which can be treated as an Eshelby inclusion [13]. In two dimensions, we develop a simple ap-

proach based upon the Kolossov-Muskhelishvili (KM) formalism of plane elasticity [14]. This is an appealing pathway to the solution since these zones will appear as poles for the potentials, and hence Cauchy integrals may easily lead to contour integral formulations which are independent of the precise contour geometry, but rather rely on its topology with respect to the different poles that are present.

Although these techniques have been mostly used in the context of numerical simulations in order to estimate stress intensity factors from finite-element simulations, they are now called for to estimate stress intensity factors from experimentally measured displacement fields from, e.g., digital image correlation techniques. In this case, interaction integral techniques [15] or least squares regression [16] techniques have been applied. Noise-robust variants have also been proposed [17]. These routes could also be followed in the present case.

Though the present work is restricted to two dimensions due to the complex potential formulation, similar questions can be addressed for the three-dimensional version of this problem using the same strategy but a different methodology. In the following, we briefly recall the KM formalism, we give analytic expressions for the contour integrals allowing us to capture the singular elastic fields, and we present a few numerical results based on a finite-element simulation supporting our analytical developments.

In Sec. II, we present the theoretical basis of our approach in terms of singular elastic fields, while in Sec. III we introduce the contour integral formulation. In Sec. IV, a numerical implementation based on finite-element simulations is presented, together with the results of the present approach. This application allows us to evaluate the performance and limitations of the contour integral procedure and check the detrimental effect of discreteness. Section V presents the main conclusions of our study.

II. POTENTIAL FORMULATION

In two dimensions, the Kolossov-Muskhelishvili potentials can be used to write the elastic stress and displacement

fields \mathbf{U} and σ [14]. Using a complex formulation, we introduce the elastic displacement $\mathbf{U} = U_x + iU_y$ and the stress tensor field through two functions, the real trace $S_0 = \sigma_{xx} + \sigma_{yy}$ and the complex function $\mathbf{S} = \sigma_{yy} - \sigma_{xx} + 2i\sigma_{xy}$. In the framework of linear elasticity, the balance and compatibility equations can be rewritten as

$$S_{0,z} - \mathbf{S}_{,\bar{z}} = 0, \quad (1)$$

$$S_{0,z\bar{z}} = 0, \quad (2)$$

where $z = x + iy$ is the complex coordinate and the notation $A_{,x}$ is used to represent the partial derivative of field A with respect to coordinate x . Note that we assumed zero surface density force and that Eq. (2) is here the classical Beltrami equation which expresses the kinematic compatibility condition in terms of stress. The general solution to these equations can be obtained through the introduction of two holomorphic functions φ and ψ , called the KM potentials. The displacement and the stress field can be written [14]

$$2\mu\mathbf{U} = \kappa\varphi(z) - \overline{z\varphi'(z)} - \overline{\psi(z)}, \quad (3)$$

$$S_0 = 2[\varphi'(z) + \overline{\varphi'(z)}], \quad (4)$$

$$\mathbf{S} = 2[\bar{z}\varphi''(z) + \psi'(z)], \quad (5)$$

where μ is the elastic shear modulus and $\kappa = (3 - 4\nu)$ for plane strain and $(3 - \nu)/(1 + \nu)$ for plane stress, ν being the Poisson ratio.

III. PLASTIC INCLUSION AND SINGULARITY APPROACH IN TWO DIMENSIONS

A. Singular terms associated with plastic inclusion

This KM formalism can be applied to two-dimensional inclusion problems [18,19]. Let us consider the case of a small inclusion of area \mathcal{A} experiencing plastic deformation and located at the origin of the coordinate system $z=0$. It is assumed that the stress is a constant at infinity. Outside the inclusion, the KM potentials can be expanded as a Laurent series as

$$\varphi(z) = \alpha^{\text{out}}z + \sum_{n=1}^{\infty} \frac{\varphi_n}{z^n}, \quad \psi(z) = \beta^{\text{out}}z + \sum_{n=1}^{\infty} \frac{\psi_n}{z^n}. \quad (6)$$

The linear terms can be easily identified as corresponding to uniform stresses while constant terms (omitted here) would lead to a rigid translation. It can be shown in addition that the dominant singular terms φ_1/z and ψ_1/z can be associated with the elastic stress induced by the plastic deviatoric and volumetric strain of an equivalent circular inclusion of area \mathcal{A} . That is, considering a circular inclusion experiencing a plastic shear strain γ_p and a plastic volumetric strain δ_p we have [18]

$$\varphi_1 = \frac{2i\mu\mathcal{A}\gamma_p}{\pi(\kappa+1)}, \quad \psi_1 = -\frac{2\mu\mathcal{A}\delta_p}{\pi(\kappa+1)}. \quad (7)$$

In particular, for a pure shear plastic event we obtain a quadrupolar symmetry:

$$\sigma_{xy} = -\frac{2\gamma_p\mu}{\kappa+1} \frac{\mathcal{A}}{\pi r^2} \cos(4\theta). \quad (8)$$

Note that we have in general to consider a complex value of γ_p to include the angular dependence of the principal axis. In contrast, the amplitude ψ_1 is a real number (note that the imaginary part would correspond to a pointlike torque applied at the origin).

B. Generic character of the expansion

Because of the well-known property of Eshelby circular inclusion, the above expansion limited to the ψ_1 and ϕ_1 terms only is the exact (outer) solution of a uniform plastic strain distributed in the inclusion, and vanishing stress at infinity. However, one should note that this result is much more general. Indeed, it is seen that the physical size of the inclusion does not enter into the solution except through the products $\mathcal{A}\gamma_p$ and $\mathcal{A}\delta_p$. Therefore, a smaller inclusion having a larger plastic strain may give rise to the very same field, provided the products remain constant. Thus one can consider the prolongation of the solution to a pointlike inclusion (with a diverging plastic strain) as being equivalent to the inclusion.

Then from the superposition property of linear elasticity, a heterogeneous distribution of plastic strain $\gamma_p(x)$ in a compact domain \mathcal{D} will give rise to such a singularity with an amplitude equal to

$$[\mathcal{A}\gamma_p]_{\text{eq}} = \int_{\mathcal{D}} \int_{\mathcal{D}} \gamma_p(x) dx \quad (9)$$

and the same property would hold separately for the volumetric part. As a particular case, one finds a uniform plastic strain for an inclusion of arbitrary shape.

This is the key property that allows us to capture the equivalent plastic strain of an arbitrary complex configuration, for the above mentioned application to amorphous media. In fact, this is even the only proper way of defining the plastic strain for a discrete medium as encountered in molecular dynamics simulations. The far-field behavior of the displacement and stress field can be accurately modeled, and without ambiguity, by a continuum approach, and thus the above result will hold. In contrast, locally, the large-scale displacement of several atoms may render difficult the direct computation of the equivalent plastic strain experienced in such an elementary plastic event.

Let us, however, stress one difficulty: As the above argument ignores the details of the action taking place within the ‘‘inclusion,’’ plasticity has to be postulated. However, a damaged inclusion, where the elastic moduli have been softened by some mechanism, or even a nonlinear elastic inclusion at one level of loading, would behave in a similar way to the above plastic inclusion. Obviously, to detect the most relevant physical description, one should have additional information, say about unloading. If the above amplitudes remain constant during unloading, plasticity would appear appropriate. If the amplitude decreases linearly with the loading, then damage is more suited. Finally, if the amplitudes varies reversibly with the loading, nonlinear elasticity might be the

best description. Thus, although one should be cautious in the interpretation, local damage detection from the far field may also be tackled with the same tools.

C. Path-independent contour integrals

In two dimensions, this multipole expansion formalism in the complex plane suggests resorting to contour integrals to extract the singularities. However, the displacement field is not a holomorphic function and cannot be used directly for that purpose. The strategy of identification of the singularities φ_n and ψ_n thus consists of expressing the potentials from the displacement field and its derivatives in order to extract the singularities via Cauchy integrals. We now simply express the displacement field and its derivatives:

$$2\mu U = \kappa\varphi(z) - z\overline{\varphi'(z)} - \overline{\psi(z)}, \quad (10)$$

$$2\mu U_{,z} = \kappa\varphi'(z) - \overline{\varphi'(z)}, \quad (11)$$

$$2\mu U_{,\bar{z}} = -z\overline{\varphi''(z)} - \overline{\psi'(z)}, \quad (12)$$

$$2\mu U_{,z\bar{z}} = -\overline{\varphi''(z)}. \quad (13)$$

This gives immediately

$$\varphi'(z) = \frac{2\mu}{\kappa-1}(\kappa U_{,z} + \overline{U_{,\bar{z}}}), \quad (14)$$

$$\varphi''(z) = -2\mu\overline{U_{,z\bar{z}}} = -\frac{\mu}{2}\overline{\nabla^2 U}, \quad (15)$$

$$\psi'(z) = -2\mu\left(\overline{U_{,\bar{z}}} - \frac{\bar{z}}{4}\overline{\nabla^2 U}\right). \quad (16)$$

Note that, except for a multiplicative constant, the two last expressions are independent of material properties. In light of the expansion (6) of φ and ψ in Laurent series, if a counterclockwise contour integration is considered along a path \mathcal{C} , Cauchy residues can be formed as

$$\varphi_n = \frac{i\mu}{4\pi n(n+1)} \int_{\mathcal{C}} z^{n+1} \overline{\nabla^2 U} dz, \quad (17)$$

$$\psi_n = \frac{i\mu}{\pi n} \int_{\mathcal{C}} z^n \left(\overline{U_{,\bar{z}}} - \frac{1}{4}\overline{z\nabla^2 U} \right) dz. \quad (18)$$

These expressions can thus be obtained from the sole knowledge of the displacement field, a quantity which can be accessed from experiments, or from atomistic simulations. In the case of first-order singularities [see Eq. (7)], the residue term thus depends only on the local plastic deformation (size and amplitude of deformation) and on the Poisson ratio ν of the material.

Reverting to Cartesian coordinates, where the contour is expressed as a function of the curvilinear abscissa s as $(x(s), y(s))$, the above expression can be written

$$\varphi_1 = \frac{\mu}{8\pi} \int_{\mathcal{C}} [-2(xy) + i(x^2 - y^2)] [(U_{x,xx} + U_{x,yy}) - i(U_{y,xx} + U_{y,yy})] \left(\frac{dx}{ds} + i \frac{dy}{ds} \right) ds,$$

$$\psi_1 = \frac{\mu}{4\pi} \int_{\mathcal{C}} \{2(ix - y)[(U_{x,x} - U_{y,y}) - i(U_{y,x} + U_{x,y})] - [i(x^2 + y^2)][U_{x,xx} + U_{x,yy} - i(U_{y,xx} + U_{y,yy})]\} \times \left(\frac{dx}{ds} + i \frac{dy}{ds} \right) ds. \quad (19)$$

IV. NUMERICAL IMPLEMENTATION

The ultimate goal of such a method would be to analyze numerical results obtained from molecular dynamics simulations of amorphous plasticity where such local structural reorganizations are expected to take place. This obviously raises the question of a well-defined method for writing the continuous displacement field from the data on the discrete displacements of particles [20] and more generally the question of the sensitivity to noise of the above expressions. The first point is beyond the scope of the present work and we leave it for later studies. We thus focus on the more restricted question of the numerical implementation and its efficiency in the case of artificially noise-corrupted displacement data.

The method relies on contour integrations of derived fields of the displacement. The latter point induces *a priori* a strong sensitivity to noise. To limit such effects, first and second derivatives are extracted via an interpolation of the local displacement field by polynomial functions of the spatial coordinates. Moreover, the path independence of the contour integrals allows one to perform spatial averages. We explore in the following the efficiency of this method for noisy data.

A. Numerical generation of elastic fields induced by plastic inclusions

Displacement fields are computed numerically using a finite-element code, with square elements and bilinear shape functions $\{1, x, y, xy\}$. Plane stress conditions of two-dimensional elasticity are used. The domain is a 150×150 square. Stress-free conditions are enforced all along the domain boundary. The Poisson ratio of the material is $\nu=0.20$. Since no quantitative values of the stress are used, the value of the Young's modulus is immaterial.

A plastic strain is implemented at the scale of one single isolated element. Within this element, the strain is the sum of a plastic uniform strain chosen at will, and an elastic strain. The latter is computed by solving for the two-dimensional elastic problem, ensuring force balance and kinematic continuity at all nodes including the nodes of the plastic element. The chosen kinematics is too crude to solve the elastic problem with a good accuracy at the scale of one single element. However, remote from the inclusion, the elastic perturbation is well accounted for, and since all our computations are

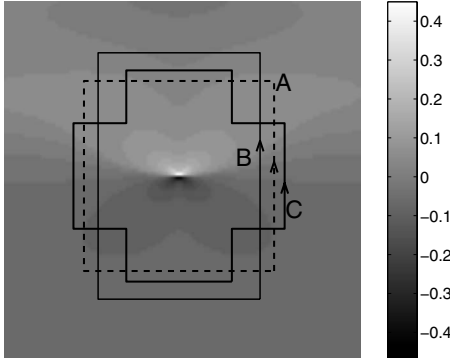


FIG. 1. Map of the displacement field U_y induced by a plastic shear strain of a central square element. The oriented paths indicate contours for integration.

based on paths lying at a distance from the inclusion, the formalism should be applicable. A single element allows us to have a maximum ratio between inclusion and domain size. The price to pay for this crude local description is that the quantitative estimate of $\mathcal{A}\gamma_p$ and $\mathcal{A}\delta_p$ will differ slightly from the theoretical expectation. Nevertheless the path independence (size, shape, center, etc.) is expected to hold.

We limited ourselves to such a description in order to mimic the difficulties one may face when having to deal with discrete element simulations. Indeed, the chosen finite-element shape functions do not allow us to use this description strictly speaking in order to compute second-order differential operators on the displacement, since the gradients of the latter are not continuous across element boundaries. Therefore, a regularization will be called for, as detailed below.

The choice of a regular square lattice is obviously oversimplified compared with the case of the random lattices associated with atomistic simulations. However, as the x and y directions are obviously equivalent for square elements and as linearity is preserved by the finite-element formulation, this formulation should not introduce any breaking of symmetry. More specifically, the displacement field induced by a quadrupole of principal direction off axis can be obtained by a linear superposition of x and y components of the displacement field induced by a quadrupole aligned with the axis weighted by the sine and cosine of the quadrupole angle.

Finally, the finite size of the system is also a specific difficulty encountered in practice, whereas the above argument uses the assumption of an infinite domain. However, such a boundary condition should not induce additional poles within the domain, and can be considered as a common practical difficulty encountered for all practical uses of this tool. All these arguments are possible causes of deviation from the theoretical expectation of path independence, and it thus motivates a detailed study of the method stability, robustness, and accuracy.

Two test cases are studied: (I) a central inclusion experiencing a shear strain $\gamma_p=1$ (because of linearity, the actual amplitude is meaningless) along the x axis; (II) a central inclusion experiencing a volumetric contraction $\delta_p=-1$. A map of the displacement fields U_y in case I is given in Fig. 1.

B. Interpolating displacement data

The key ingredient is to go from a continuous but nondifferentiable displacement field obtained from the finite-element simulation to an evaluation of the second derivative at any point in the domain. The results presented below have been obtained using the following procedure. A quadratic fit is performed on a square centered on one node to extract the first- and second-order derivatives, and the obtained values are used to compute the integrals by quadrature. An alternative method has been tested: for an integration from (x, y) to $(x+1, y)$, a simple fit is performed of the 12 nodes ranging from $(x-1, y)$ to $(x+2, y)$, and from $(y-1)$ to $(y+1)$, by the tensor product of polynomials $(1, x, x^2, x^3)$ and $(1, y, y^2)$ (12 functions). Then the integral of all required quantities can be computed. Estimates of derivatives using Fourier series with and without low-pass filtering have also been performed. All methods give similar results provided that the area of the region used for interpolation (or filtering) is comparable.

C. Path independence

We first check the path independence of the contour integral in the cases I and II of isolated inclusions. For that purpose, we use three families of contours, square (A), cross (B), and rectangular (C) shaped respectively as shown in Fig. 1. The size of these contours as well as their center can be varied. Figure 2 gives a summary of the results. For the three kinds of contours, we show the real and imaginary parts of the residues corresponding to Eq. (17). Note that the numerical results have been normalized according to the theoretical expectations (7) so that the expected numerical values are $\varphi_1=i, \psi_1=0$ in case I (Fig. 2, left) and $\varphi_1=0, \psi_1=1$ in case II (Fig. 2, right).

These numerical results can be considered as rather satisfactory in terms of orientation and orthogonality between modes φ_1 and ψ_1 : the measured values of quantities whose expected value is zero remain typically below 10^{-2} . When compared to their theoretical values, φ_1^{shear} and $\psi_1^{\text{contraction}}$ exhibit relative differences of around 5–10%. Small fluctuations (below 5%) can be found when the shape and size of the contours are varied. We already commented on the fact that the finite-element simulations are performed with a single element for the inclusion, a procedure which is obviously not reliable in terms of accuracy, but which allows us to have a large ratio between element and system size.

Another test of the numerical procedure is its dependence on the sole topology, i.e., location of the inclusion inside or outside the contour; we show in addition the dependence of the measured values of φ_1 and ψ_1 on the location of the contour center. Figure 3 shows the singularity ψ_1 measured from the integration of displacement field II along a square contour centered along the x axis. Results are normalized so that the expected value of $\text{Re}\psi_1$ is unity when the inclusion is within the contour and zero elsewhere. The contour size is $M=20$. We obtain the expected behavior: the values of $\text{Re}\psi_1$ shift from zero to unity depending on whether the inclusion is within or outside the contour. Significant fluctuations (10–20%) are, however, observed when the inclusion lies in the vicinity of the contour.

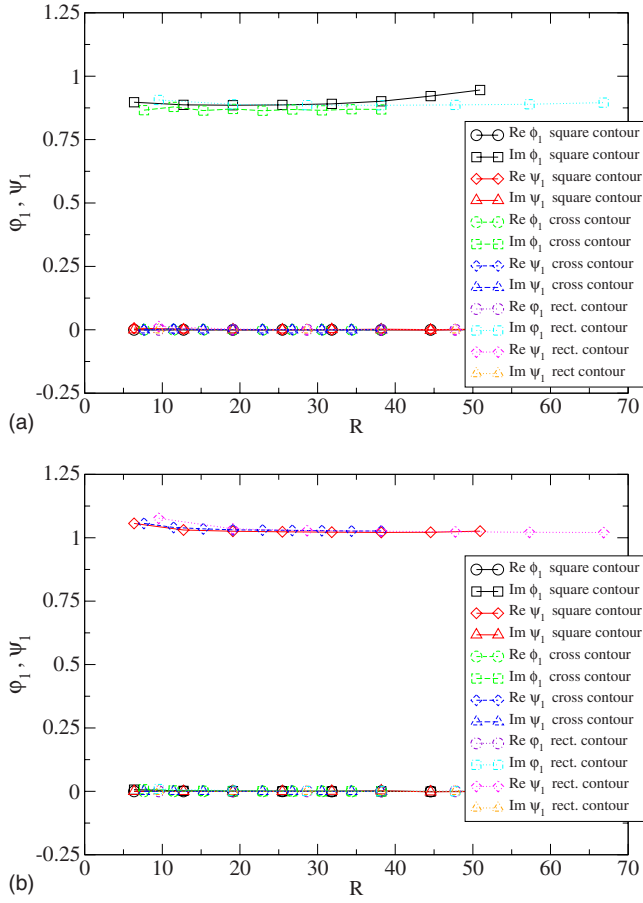


FIG. 2. (Color online) Normalized values of numerical estimates ϕ_1 and ψ_1 obtained for three families of contours, respectively square, cross, and rectangle shaped, and of varying length L in the case of a displacement field induced by the plastic shear strain (left) or contraction (right) experienced by the central element of a square lattice. Theoretical expectations are $\phi_1=i, \psi_1=0$ (left) and $\phi_1=0, \psi_1=1$ (right).

Finally we test the dependence of the numerical method on the material properties. In the determination of ϕ_1 and ψ_1 (17) as residues, the need to resort to a second-order derivative of the displacement field is balanced by the fact that the computation can be performed without any knowledge of the elastic properties of the material. The lack of dependence of the numerical procedure on the Young's modulus is trivially obtained due to the linearity of the finite-element method (FEM) computation. In Fig. 4 we show the dependence of the numerical results on the Poisson ratio. FEM computations have been performed on systems of size 100×100 with stress-free boundary conditions and a central inclusion experiencing a unit shear and a unit contraction, respectively. The Poisson ratio was varied from 0.05 to 0.45 by steps of 0.05. The results shown in the figure compare the numerical estimates obtained for a square contour of size 40 centered on the inclusion with the theoretical expectation $\psi_1 = \phi_1 = (1 + \nu)/2\pi$. The numerical results show that the volumetric strain is weakly dependent on the Poisson ratio, but the elementary shear is more poorly estimated for a high Poisson ratio.

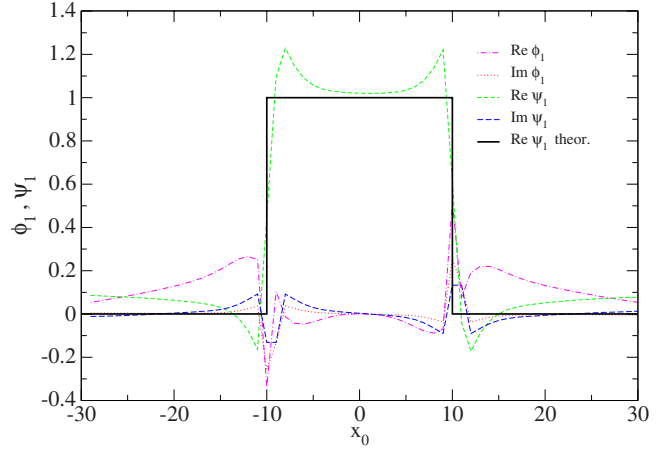


FIG. 3. (Color online) Normalized values of numerical estimates ϕ_1 obtained for square contours of center $(x_0, 0)$ and size $M=20$. The expected behavior of $\text{Re } \psi_1$ (unity when the inclusion lies within the contour, zero otherwise) is represented by the bold line. Other quantities are expected to be zero.

V. DISCUSSION AND CONCLUSION

The proposed approach is based on an exact result and hence theoretically establishes a parallel with other types of elastic singularities (in particular the stress intensity factors which characterize crack loadings) where similar path integrals are well known. When tested on direct numerical simulations, we could recover the main topological properties expected in this context: path independence and detection of the absence or presence of a singularity within the contour. However, the quantitative results proved more disappointing: the method is rather imprecise in the determination of the prefactor of the singularity and is more generally rather sensitive to noise. The main cause is presumably the inconsistent regularity of the displacement field solution (simple con-

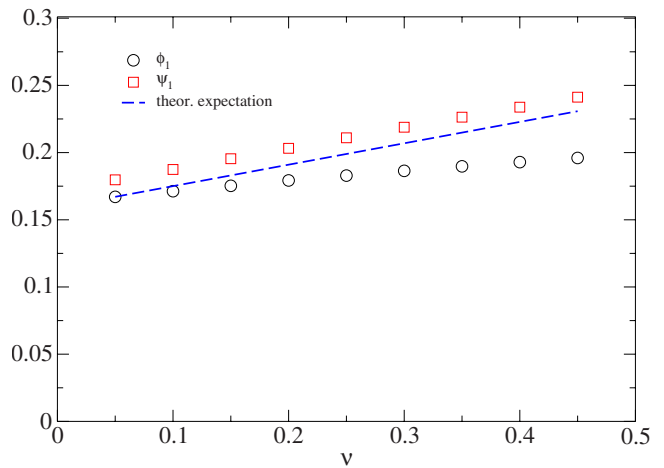


FIG. 4. (Color online) Numerical estimates of $|\phi_1|$ and ψ_1 obtained for a central inclusion experiencing a unit shear and a unit contraction, respectively, as a function of the Poisson ratio ν . The numerical results obtained in plane stress conditions for a system of size 100×100 with stress-free boundary conditions are compared with the theoretical expectation $(1 + \nu)/2\pi$.

tinuity) with the need to resort to estimates of first- and second-order differentials. A piecewise high-order polynomial interpolation is operational for integrals over finite segments; however, from one segment to the next, first- and second-order differentials will display a discontinuous character, which obviously affects the method and results. Moreover, being a path integral, the method does not take advantage of the knowledge of the displacement field at all points of a domain. To make the method more robust with respect to noise, different approaches can be followed. One natural way is to average the result over different contours, thus transforming the contour integral into a domain integral. An arbitrary weight average can also be considered, and hence one could optimize the weight in order to achieve the least

noise sensitivity. Such a method was explored successfully for cracks in Ref. [17]. Note finally that extensions to three dimensions obviously require a different technique from Kolosov-Muskhelishvili potentials and contour integrals; however, a linear extraction operator acting on the displacement field can still be computed to provide similarly the equivalent plastic strain.

ACKNOWLEDGMENTS

V.P. acknowledges the financial support of ANR program “PlastiGlass” Grant No. NT05-4_41640 and of the Academy of Finland.

-
- [1] V. V. Bulatov and A. S. Argon, *Modell. Simul. Mater. Sci. Eng.* **2**, 167 (1994).
 [2] V. V. Bulatov and A. S. Argon, *Modell. Simul. Mater. Sci. Eng.* **2**, 185 (1994).
 [3] V. V. Bulatov and A. S. Argon, *Modell. Simul. Mater. Sci. Eng.* **2**, 203 (1994).
 [4] M. L. Falk and J. S. Langer, *Phys. Rev. E* **57**, 7192 (1998).
 [5] J.-C. Baret, D. Vandembroucq, and S. Roux, *Phys. Rev. Lett.* **89**, 195506 (2002).
 [6] G. Picard, A. Ajdari, F. Lequeux, and L. Bocquet, *Phys. Rev. E* **71**, 010501(R) (2005).
 [7] A. Lemaître and C. Caroli, e-print arXiv:cond-mat/0609689v1.
 [8] E. A. Jagla, *Phys. Rev. E* **76**, 046119 (2007).
 [9] M. Zaiser and P. Moretti, *J. Stat. Mech. Theory Exp.* (2005) P08004.
 [10] A. Tanguy, F. Leonforte, and J.-L. Barrat, *Eur. Phys. J. E* **20**, 355 (2006).
 [11] C. E. Maloney and A. Lemaître, *Phys. Rev. E* **74**, 016118 (2006).
 [12] J. Rice, *J. Appl. Mech.* **35**, 379 (1968).
 [13] J. D. Eshelby, *Proc. R. Soc. London, Ser. A* **241**, 376 (1957).
 [14] N. Muskhelishvili, *Some Basic Problems of the Mathematical Theory of Elasticity* (Noordhoff, Groningen, 1953).
 [15] J. Réthoré, A. Gravouil, F. Morestin, and A. Combescure, *Int. J. Fract.* **132**, 65 (2005).
 [16] S. Roux and F. Hild, *Int. J. Fract.* **140**, 141 (2006).
 [17] J. Réthoré, S. Roux, and F. Hild, *Eng. Fract. Mech.* **75**, 3763 (2008).
 [18] M. Jawson and R. Bhargava, *Proc. Cambridge Philos. Soc.* **57**, 669 (1961).
 [19] J. Mathiesen, I. Procaccia, and I. Regev, *Phys. Rev. E* **77**, 026606 (2008).
 [20] I. Goldhirsch and C. Goldenberg *Eur. Phys. J. E* **9**, 245 (2002).